Heliyon 9 (2023) e17751

Contents lists available at ScienceDirect

Heliyon

journal homepage: www.cell.com/heliyon

Analysis of the Time-Dependent magnetohydrodynamic Newtonian fluid flow over a rotating sphere with thermal radiation and chemical reaction

Showkat Ahmad Lone [a], Sadia Anwar [b], Zehba Raizah [c], Poom Kumam [d,**], Thidaporn Seangwattana [e,*], Anwar Saeed [d]

[a] Department of Basic Sciences, College of Science and Theoretical Studies, Saudi Electronic University (Jeddah-M), Riyadh, 11673, Kingdom of Saudi Arabia
[b] Department of Mathematics, College of Arts and Sciences, Wadi Ad Dawasir, 11991, Prince Sattam Bin Abdulaziz University, Al-Kharj, Kingdom of Saudi Arabia
[c] Department of mathematics, college of Science, Abha, King Khalid University, Saudi Arabia
[d] Center of Excellence in Theoretical and Computational Science (TaCS-CoE), Science Laboratory Building, Faculty of Science, King Mongkut's University of Technology Thonburi (KMUTT), 126 Pracha-Uthit Road, Bang Mod, Thung Khru, Bangkok, 10140, Thailand
[e] Department of Science Energy and Environment, King Mongkut's University of Technology North Bangkok, Rayong Campus (KMUTNB), 21120, Rayong, Thailand

ARTICLE INFO

Keywords:
Nanofluid
Rotating sphere
Stagnation point
Brownian motion and thermophoresis
MHD
Viscous dissipation
HAM

ABSTRACT

This article presents the magnetohydrodynamic (MHD) flow of a nanoliquid due to a rotating sphere at a stagnation point. The flow is considered to be influenced by the magnetic field, dissipative, thermally radiative, and chemically reactive. Also, the thermophoretic and Brownian motion influences are taken into consideration. Some restrictions in the present analysis are taken: like there is no-slip and convective conditions, joule heating, Hall effects and buoyancy-driven. The solution of the present analysis is derived through the homotopy analysis method (HAM). The significance of several physical parameters on velocities, thermal and concentration profiles are shown with the help of Figures. Also, the significance of different physical factors on skin frictions, local Nusselt number and Sherwood number are demonstrated with the help of Tables. The outcomes show that the Nusselt number is lower for the larger Brownian motion parameter, Eckert number, and thermophoretic parameter, while the increment in the thermal radiation parameter augmented the Nusselt number. It is established that the increasing rotation, magnetic and positive constant parameters have increased the velocity profiles along the *x*-direction while reducing the velocity profiles along the z-direction of the nanoliquid flow. The increasing positive constant parameter reduces the thermal graph of the nanoliquid flow. Furthermore, the intensifying Eckert number, thermophoresis, Brownian motion, and thermal radiation factor have escalated the thermal profiles of the nanoliquid flow.

* Corresponding author.
** Corresponding author. Department of Medical Research, China Medical University Hospital, China Medical University, Taichung, 40402, Taiwan.
E-mail addresses: poom.kum@kmutt.ac.th (P. Kumam), thidaporn.s@sciee.kmutnb.ac.th (T. Seangwattana).

https://doi.org/10.1016/j.heliyon.2023.e17751
Received 17 February 2023; Received in revised form 26 June 2023; Accepted 27 June 2023
Available online 4 July 2023

Nomenclature

angular velocity $\Omega(t) = \frac{b}{t}$
Surface temperature T_w
Thermophoresis diffusion D_T
Chemical reaction rate C_r
Stefan-Boltzmann constant σ^*
Thermal radiation factor Rd
Schmidt number Sc
Reynolds number Re
Thermophoretic factor Nt
Eckert number Ec
Brownian diffusion D_B
Nanoparticles density $(\rho)_{np}$
Specific heat C_p
Density ρ
Velocity components u, v and w
Magnetohydrodynamic MHD
free-stream velocity $U(x,t) = \frac{ax}{t}$
Magnetic field $B = \frac{B_0}{\sqrt{\gamma t}}$
Surface concentration C_w
Absorption factor k^*
Magnetic parameter M
Prandtl number Pr
Rotation factor R
Skin friction C_{fx}
Brownian motion factor Nb
Chemical reaction factor C_R
Thermal conductivity k
Specific heat of nanoparticles $(C_p)_{np}$
Ambient velocity U
radial distance r
Dynamic viscosity μ
Homotopy analysis method HAM

1. Introduction

Magnetohydrodynamic is the study of those fluids which are conducted electrically such as liquid metal and plasma etc. The theory of MHD was the idea of Hannes Alfven. Many investigations have been established with the main emphasis on the influence of MHD over heat transmission characteristics and motion of the fluid. Asjad et al. [1] analyzed viscous MHD liquid flow on a sheet using power law fractional differential operators. Vaidya et al. [2] evaluated the MHD liquid flow in a contracting asymmetric medium and determined that greater estimates of magnetic factors have caused a jump in thermal flow profiles and a reduction in a fluid motion. Reddy et al. [3] determined the upshot of chemical reactions and radiations on MHD liquid motion past an elongating surface and have established that fluid motion, Nusselt, Sherwood numbers and skin friction have declined with enlargement in the magnetic effects. Fenizri et al. [4] have used a modified technique for the solution of MHD liquid flow through a channel and have elaborated the consequence of magnetic field upon flow profiles. Ali et al. [5] and Saeed et al. [6] evaluated the thermophysical characteristics of a base fluid containing Al2O3 Nano particulates of various shapes in the energy transmission of an erratic thin film flow across an extended surface. According to the study, Al2O3 nano granules have a rapid rate of heat and flow transmission. Khan et al. [7] dissected the significance of Marangoni convection on MHD hybrid nanoparticle flow upon an elongating sheet. Kodi and Mopuri [8] have studied time-based MHD liquid flow on a vertically inclined surface by employing chemically reactive heat absorption effects. Rehman et al. [9] have deliberated on thermal flow for MHD Jeffery fluid over a cylindrical surface subject to the impact of radiation. Abbas et al. [10,11]numerically examined the behavior of radiative flow of a conductive viscous fluid through a permeable surface with the slip effects and found that the energy field increases, while the fluid's velocity decreases due to the Lorentz force.

Brownian motion and thermophoretic phenomena are the thermal and mass transportation movements of small particles using falling concentration and thermal gradients. These effects disturb the movements of tiny particles in the closed vicinity of bulk surfaces of the medium. It has plenty of applications in different areas such as aerospace, nuclear safety process, atmosphere pollution and aerosol technologies, etc. Mittal and Patel [12] have discussed mixed convective MHD Casson fluid flow using nonlinear radiative heat generation, subject to Brownian and thermophoresis effects and have exposed that both Brownian and thermophoresis factors have a

negative impact on the thermal gradient. Riaz et al. [13] developed the Cattaneo-Christov thermal flux model for the nonlinear conduction of Walter-B nanoliquid owing to an extended surface with the effect of a non-uniform heat source. Sabir et al. [14] studied the influences of Brownian motion and thermophoretic diffusion upon time-dependent micropolar nanoparticle flow on an extending sheet. Guderi et al. [15] have applied the idea of tri-hybrid nanoliquid past a nonlinear stretched surface by employing the Darcy-Forchheimer model and have established that temperature distribution have upsurge and concentration diffusions have weakened with growth in Brownian factor. Abdelsalam et al. [16] described the sinusoidal channel's electromagnetism field, chemical change, and electro osmotic flow of non-Newtonian hybrid nanoliquid flow. It was discovered that the laser factor effect improves thermal transfer and fluid flow. Sridhar et al. [17] reviewed the effects of diamond and copper tiny particles on a vertical microchannel-based electro-magneto-hydrodynamic nanoliquid flow. The couple stress factor was found to decrease velocity while increasing the shear stress and pressure gradient of the nanofluid. Khan et al. [18] have examined thermally the nanoliquid flow under a porous surface using the influence of gyrotactic microorganisms. Mabood et al. [19] have considered Brownian and thermophoresis characteristics over thermally radiative fluid flow near a constantly flat moving plate. Upreti et al. [20] deliberated the influences of thermophoretic and Brownian diffusivity upon Casson nanoparticles flow over a Riga plate subject to the impact of microorganisms. Rasheed et al. [21,22] evaluated the effects of Brownian motion, thermophoresis, and thin-film nanoparticles motion over elastic spinning inclined surface. Zeeshan and Shaikh [23] investigated how time-dependent viscosity and nanoparticles affected the third-grade fluid's thermal and mass transportation systems during cable encasing mechanism in the presence of a magnetic field.

In many phenomena such as vaporization, absorption, thermal insulations, food processing, cooling towers, condensation in a mixture, etc. the transmission of mass is a natural process. In most living-matter phenomena like sweating, nutrition, and respiration mass transmission is a major factor. Chemical reactions have been given special attention in all such processes in the recent past due to their significance in many chemical engineering processes. Rasool et al. [24] have discussed the influences of thermally radiative chemical reactions over Darcy-Forchheimer nanofluid flow on a stretching surface and have established that radiation and chemical factors have a strong impact on thermal distribution. Khan et al. [25] researched the effects of the chemical reactions and the convective thermal transfer through the Casson fluid induced by moving wedge submerged in a permeable material. It was determined that the unsteadiness component reduced the thermal boundary layers while thinning the velocity field. Zainal et al. [26] presented the thermal fluid flow for hybrid nanoliquid upon a porous movable wedge using the impact of chemically reactive activation energy. Cui et al. [27] have studied different models for forced convective nanoliquid flow over an elongating surface subject to chemical reactions and heat production sources. Raza et al. [28] and Faizan et al. [29] studied the radiative Sutterby flow of nanoliquid over an extensible cylinder and came to the conclusion that the increase in the Brownian motion variable raises the internal temperature of the fluid. Salahuddin et al. [30] have inspected squeezing Maxwell fluid flow through an infinite channel using the impact of chemical reactions and have concluded that the fluid motion has been opposed strongly by growth in the chemical reaction due to which concentration has declined. Dey et al. [31] have analyzed the stability of dual solutions for MHD fluid flow upon porous extending surface subject to chemical reactions and thermal radiations. By using engine oil as the functioning fluid, Zeeshan [32] examined the flow of a Maxwell nanoliquid containing graphene and molybdenum disulfide Nano particulates with ramped and isothermal wall temperature. Rasheed et al. [33] employed computational methods to explain the steady 2D MHD free convection flow of Casson nanoliquid over a horizontal surface while taking into account the effects of chemical reaction and thermal radiation. Wang et al. [34] have discoursed the optimization of irreversibility for Darcy-Forrchheimer model-based viscous fluid flow upon a curved surface with the influence of chemical reactions on a liquid flow system. Similar investigations can be studied in Refs. [35–39].

The motion-induced due to the spinning of a sphere or spherical particles can be seen in various applications of engineering such as metrology and fluid dynamics in science etc. The motivation in the present study is to consider fluid motion induced by a rotary sphere and then to estimate different characteristics of resultant fluid flow. Many investigations can be seen in literature comprising fluid motion due to rotating spheres. Mahdy et al. [40] analyzed the production of irreversibility and time-based convective stagnation point MHD flow around a rotary sphere and it has established in this study that temperature distribution has enlarged with growth in a magnetic field, rotation of the sphere, and acceleration of free stream. Later Mahdy and Nabwey [41] added the impact of microorganisms in their early investigation [40]. Ali et al. [42] dissected the significance of MHD nanoliquid flow at the stagnant point of the spinning sphere and concluded that progression in the rotary sphere factor has expanded the fluid motion in the x-direction. Patil et al. [43] have debated the influences of convective nanoparticles flow past a spinning sphere with the impact of fluid hydrogen diffusions. Ramesh et al. [44] studied the CNT's hybrid nanoliquid flow due to the spinning sphere using the upshot of thermal radiations and deposition of particles. Dawar and Acharya [45] have discussed the time-based nanofluid flow at the stagnant point of the gyrating sphere. Mahmood et al. [46] evaluated the time-dependent tri-hybrid liquid flow past a rotary sphere using Joule heating and magnetic effects. Abbas et al. [47–49]analyzed the hybrid nanoliquid flow through a porous curled surface with irregular extending using the numerical approach bvp4c. In the case of injection, the energy profile shows a declining behavior for raising the particle concentration, whereas in the case of suction, the energy profile increases for raising the concentration of nano particulates.

The impact of viscous dissipation is normally ignored by many researchers; however, its existence becomes substantial whenever the viscosity of the liquid is too high. Its presence alters the thermal distribution by acting as an energy source in the fluid flow phenomenon which affects the rate of heat transmission and ultimately influences the fluid flow system. Rajakumar et al. [50] have reviewed the MHD viscous dissipative flow of liquid on an infinitely extended flat permeable plate using ion slip current and exposed that velocity distribution has weakened with progression in Schmidt number and Casson factor but augmentation in ion slip factor has upsurge the motion of the fluid. Megahed and Reddy [51] have studied numerically the MHD liquid flow using viscous dissipation and variable fluid characteristics on an extending surface. Gopal et al. [52] numerically examined MHD fluid flow subject to the impact of viscous dissipation past a linear stretched sheet and have exposed that progression in magnetic effects has declined the liquid velocity but upsurge the thermal flow of fluid. Abbas and Megahed [53] have discussed the significance of chemically reactive viscous

dissipation due to the MHD liquid flow upon a stretching sheet. Nadeem et al. [54] discussed the second-grade nanoliquid flow over an extensible vertical Riga surface with varying thicknesses. Variable thermal conductivity and viscosity are considered that depend on temperature, and changes in concentration and temperature are also noted when thermal and mass time relaxation factor rises. Shatanawi et al. [55] studied thermophoresis, molecular diffusion effects, and employed the generalized Fick's and Fourier law for Second-grade fluid flow at a narrow upward Riga sheet. It was concluded that the thermophoresis effect has a rising effect on the energy curves. Yaseen et al. [56] have considered liquid flow over a permeable surface subject to the impact of viscous dissipation and suction/injection. Kataria et al. [57] studied EMHD fluid flow using viscous dissipation and nonlinear radiations past a linearly extended surface with slip conditions. Sharma et al. [58] simulated numerically the heat and mass transportation for MHD liquid flow upon a spinning disk with the impact of viscous dissipation. Arafa et al. [39] reviewed the nanoliquid flow through a penetrable media subject to the impact of heat generation. Hayat et al. [40] exposed the upshot of melted heat and viscous dissipation over hybrid nanoliquid flow due to the parallel plates and exposed that fluid motion has expanded with progression in Reynolds number and squeezing factor. An artery with three distinct specifications; converging, diverging, and non-tapered was used by Bhatti and Abdelsalam [59], to study the interaction of tantalum and cobalt nanoparticles in a hybrid fluid model.

In the present investigation, the authors have investigated the MHD stagnation point flow of a nanoliquid due to the rotating sphere. The flow is considered to be influenced by the magnetic field, dissipative, thermally radiative, and chemically reactive. Also, the thermophoretic and Brownian motion influences are taken into consideration. Some restrictions in the present analysis are taken: like there is no-slip and convective conditions, joule heating, Hall effects and buoyancy-driven. This analysis is composed of problem formulation which is presented in Section 2. HAM solution is presented in Section 3. The results and discussion of the present analysis is presented in Section 4. The final points are presented in section 5.

2. Problem formulation

Consider the unsteady, laminar and incompressible flow of a magnetohydrodynamic nanoliquid at the stagnation point of a rotating sphere that rotates with an angular velocity $\Omega(t) = \frac{b}{t}$ where $t > 0$ and $b > 0$. The free-stream velocity of the nanofluid flow is defined by $U(x,t) = \frac{ax}{t}$. The coordinate axes are chosen that the $x-$ axis is along the surface of the sphere and $y-$ axis is chosen perpendicular the surface of the sphere. Along $y-$ axis, a magnetic field of strength $B = \frac{B_0}{\sqrt{\gamma t}}$ is imposed. The surface of the rotating sphere is kept with constant temperature T_w and concentration C_w. T_∞ and C_∞ are the ambient temperature and concentration correspondingly. Some restrictions in the present analysis are taken: like there is no-slip and convective conditions, joule heating, Hall effects and buoyancy-driven. Some phenomena are considered in the present analysis which is listed as:

- Magnetically influenced
- Stagnation point region
- Thermally radiative and dissipative
- Brownian motion and thermophoresis
- Chemical reaction

Therefore, based on the above observations, the governing equations are discoursed as.

$$\frac{\partial(ru)}{\partial x} + \frac{\partial(rv)}{\partial y} = 0, \tag{1}$$

$$\left(\frac{\partial u}{\partial t} + u\frac{\partial u}{\partial x} + v\frac{\partial u}{\partial y} - \left(\frac{w^2}{r}\right)\frac{\partial r}{\partial x}\right) = \frac{\partial U}{\partial t} + U\frac{\partial U}{\partial x} + \frac{\mu}{\rho}\frac{\partial^2 u}{\partial y^2} + \frac{\sigma B_0^2}{\rho}(u - U), \tag{2}$$

$$\left(\frac{\partial w}{\partial t} + u\frac{\partial w}{\partial x} + v\frac{\partial w}{\partial y} + \left(\frac{uw}{r}\right)\frac{\partial r}{\partial x}\right) = \frac{\partial^2 w}{\partial y^2} - \frac{\sigma B_0^2}{\rho}B_0^2 w, \tag{3}$$

$$\frac{\partial T}{\partial t} + u\frac{\partial T}{\partial x} + v\frac{\partial T}{\partial y} = \frac{k}{\rho C_p}\frac{\partial^2 T}{\partial y^2} - \frac{1}{\rho C_p}\frac{16\sigma^* T_\infty^3}{k^*}\frac{\partial^2 T}{\partial y^2} + \frac{(\rho C_p)_{np}}{\rho C_p}\left(D_B\frac{\partial C}{\partial y}\frac{\partial T}{\partial y} + \frac{D_T}{T_\infty}\left(\frac{\partial T}{\partial y}\right)^2\right) + \frac{\mu}{\rho C_p}\left(\frac{\partial u}{\partial y}\right), \tag{4}$$

$$\left(\frac{\partial C}{\partial t} + u\frac{\partial C}{\partial x} + v\frac{\partial C}{\partial y}\right) = D_B\frac{\partial^2 C}{\partial y^2} + \frac{D_T}{T_\infty}\frac{\partial^2 T}{\partial y^2} - C_r(C - C_\infty), \tag{5}$$

with boundary conditions:

$$\left\{\begin{array}{l} \text{for} \quad t < 0 : u = 0, v = 0, w = 0, T = T_\infty, C = C_\infty. \\ At \quad y = 0 : t > 0, u = 0, v = 0, w = r\Omega(t), T = T_w, C = C_w. \\ When \quad y \to \infty : u \to U, w \to 0, T \to T_\infty, C \to C_\infty. \end{array}\right\} \tag{6}$$

Here along $x-$, $y-$ and $z-$ directions the velocity components are u, v and w, correspondingly, μ is the dynamic viscosity of the nanofluid, ρ is the density of the nanofluid, r is the radial distance, t is the time, the specific heat of the nanoliquid is C_p, U displays the

ambient velocity, $(\rho)_{np}$ is the nanoparticles density, the specific heat of the nanoparticles is $(C_p)_{np}$, the nanofluid thermal conductivity is k, the temperature is T, the Brownian diffusion coefficient is D_B, the thermophoretic diffusion coefficient is D_T, the Stefan-Boltzmann constant is σ^*, k^* is the absorption factor, C_r is the reaction rate and Ω is the angular velocity.

The similarity variables are defined as [60]:

$$\left.\begin{array}{l} r \approx x, \dfrac{dr}{dx} = 1, \chi = \sqrt{\dfrac{2y^2}{\nu t}}, u = \dfrac{ax}{t}F^{'}(\chi), v = -\sqrt{\dfrac{2\nu}{t}}aF(\chi), \\ w = \dfrac{bx}{t}G(\chi), T = T_\infty + (T_w - T_\infty)\theta(\chi), C = C_\infty + (C_w - C_\infty)\varphi(\chi). \end{array}\right\} \tag{7}$$

By applying of above-mentioned similarity variables, equation (1) is obvious and equations (2)–(6) are transformed as:

$$\begin{array}{l} F^{'''}(\chi) + aF(\chi)F^{''}(\chi) + 0.5a\left(1 - (F^{'}(\chi))^2 + R(G(\chi))^2\right) \\ \quad -0.5(1 - F^{'}(\chi) - 0.5\chi F^{''}(\chi)) + M(1 - F^{'}(\chi)) = 0, \end{array} \tag{8}$$

$$G^{''}(\chi) + a(FG^{'} - GF^{'}) + 0.5(G + 0.5\chi G^{'}) - MG = 0, \tag{9}$$

$$\frac{1}{\Pr}(1 + Rd)\theta^{''}(\chi) + af^{'}(\chi)\theta^{'}(\chi) + 0.25\theta^{'}(\chi) + Nb\theta^{'}(\chi)\varphi^{'}(\chi) + Nt(\theta^{'}(\chi))^2 + Ec(F^{''}(\chi))^2 = 0, \tag{10}$$

$$\varphi^{''}(\chi) + \frac{Nt}{Nb}\theta^{''}(\chi) + aScf^{'}(\chi)\varphi^{'}(\chi) + 0.25\varphi^{'}(\chi) - 0.5C_R\varphi^{'}(\chi) = 0, \tag{11}$$

$$\left.\begin{array}{l} F(\chi = 0) = 0, F^{'}(\chi = 0) = 0, F^{'}(\chi \to \infty) \to 1, G(\chi = 0) = 1, G(\chi \to \infty) \to 0, \\ \theta(\chi = 0) = 1, \theta(\chi \to \infty) \to 0, \varphi(\chi = 0) = 1, \varphi(\chi \to \infty) \to 0. \end{array}\right\} \tag{12}$$

where

$$\left.\begin{array}{l} M = \dfrac{\sigma B_0^2}{\rho\gamma}, Rd = \dfrac{16\sigma^* T_\infty^3}{3kk^*}, \Pr = \dfrac{\mu C_p}{k}, Sc = \dfrac{\nu}{D_B}, R = \dfrac{b}{a}, \\ Nt = \dfrac{(\rho C_p)_{np} D_B (C_w - C_\infty)}{\nu(\rho C_p)}, Nb = \dfrac{(\rho C_p)_{np} D_T (T_w - T_\infty)}{\nu T_\infty (\rho C_p)}, C_R = \dfrac{C_r}{a}. \end{array}\right\} \tag{13}$$

In equations (8)–(11), the magnetic parameter is denoted by M, Rd shows thermal radiation factor, Pr shows the Prandtl number, Sc indicates the Schmidt number, the chemical reaction factor is indicated by C_R, R represents the rotation factor, Ec indicates the Eckert number, Nt shows the thermophoretic factor and Nb indicates the Brownian motion factor.

The quantities of interest like skin friction, Nusselt number and Sherwood number are defined as:

$$C_{fx} = \frac{2\tau_{wx}}{\rho U^2}, C_{fz} = \frac{2\tau_{wz}}{\rho U^2}, Nu_x = \frac{xq_w}{k(T_w - T_\infty)}, Sh_x = \frac{xq_m}{D_B(C_w - C_\infty)}, \tag{14}$$

where

$$\tau_{wx} = \left.\frac{\partial u}{\partial y}\right|_{y=0}, \tau_{wz} = \left.\frac{\partial w}{\partial y}\right|_{y=0}, q_w = -k\left(\frac{\partial T}{\partial y} + q_r\right)\Big|_{y=0}, q_m = -D_B\left.\frac{\partial C}{\partial y}\right|_{y=0}, \tag{15}$$

Thus, we have,

$$\left.\begin{array}{l} C_{fx}\mathrm{Re}_x^{1/2} = \dfrac{1}{\sqrt{a}}F^{''}(\chi = 0), C_{fz}\mathrm{Re}_x^{1/2} = \dfrac{1}{\sqrt{a}}G^{'}(\chi = 0), \\ Nu_x\mathrm{Re}_x^{-1/2} = -(1 + Rd)\theta^{'}(\chi = 0), Sh_x\mathrm{Re}_x^{-1/2} = \varphi^{'}(\chi = 0), \end{array}\right\} \tag{16}$$

where the local Reynolds number is $\mathrm{Re}_x = \frac{ax^2}{\nu}$.

3. HAM solution

The initial guesses and linear operators are deliberated as:

$$F_0(\chi) = \chi - 1 + Exp(-\chi), G_0(\chi) = Exp(-\chi), \theta_0(\chi) = Exp(-\chi), \varphi_0(\chi) = Exp(-\chi), \tag{17}$$

$$L_F = F^{'''} - F^{'}, L_G = G^{''} - G, L_\theta = \theta^{''} - \theta, L_\varphi = \varphi^{''} - \varphi, \tag{18}$$

with

$$\left\{\begin{array}{l} L_F(\xi_1+\xi_2\,Exp(-\chi)+\xi_3\,Exp(\chi))=0, \\ L_G(\xi_4\,Exp(-\chi)+\xi_5\,Exp(\chi))=0, \\ L_\theta(\xi_6\,Exp(-\chi)+\xi_7\,Exp(\chi))=0, \\ L_\varphi(\xi_8\,Exp(-\chi)+\xi_9\,Exp(\chi))=0, \end{array}\right\} \tag{19}$$

where $\xi_n(n=1-9)$ are the constants (see Table 1) (see Fig. 1).

4. Results and discussion

In this section, we have discussed the impacts of the physical factors on the profiles of the unsteady, laminar and incompressible flow of a magnetohydrodynamic nanoliquid at stagnation point of a rotating sphere. The present analysis is verified by comparing the present results with published results of Ramesh et al. [44] and Malvandi [61] for different values of a. A great agreement between the present and published results is found which verify the correctness of the present model. The effects of embedded factor on the skin frictions along $x-$ and $z-$ directions, local Nusselt number, and Sherwood number are presented in Tables 2–5. Also, the impacts of the embedded factors on velocities, thermal and concentration profiles are displayed in Figs. 2–7. Table 2 signifies the results of the constant parameter a, rotating parameter R, and magnetic parameter M on the skin friction coefficient C_{fx} in $x-$ direction. In Table 2, the declining role of C_{fx} of the liquid in $x-$ direction is examined for higher estimates of the constant parameter a, rotating parameter R, and magnetic parameter M. The consequence of constant parameter a on the skin friction coefficient C_{fz} in $z-$ direction is determined in Table 3. It is eminent that with the increase of the constant parameter a, the C_{fz} in $z-$ direction is diminishing. The role of the thermal radiation parameter Rd, Eckert number Ec, Brownian motion parameter Nb, and thermophoresis parameter Nt on the Nusselt number Nu_x of the fluid is analyzed in Table 4. In this evaluation, the fluid Nusselt number Nu_x is lower for higher Ec, Nb, and Nt but increment in Rd augmented the Nu_x of the nanofluid. Table 5 is presented to determine the consequence of the thermophoresis parameter Nt, Brownian motion parameter Nb, and chemical reaction parameter C_R on the Sherwood number Sh_x. It is noticed that the Sh_x of the nanoliquid is enhances due to the increase of the Nt and C_R. Further, the decayed behavior of Sh_x of the nanofluid is noted when Nb is enhances. The outcomes of constant parameter a, magnetic parameter M and rotating parameter R on the velocity profile in $x-$ direction are discussed in Fig. 2. Fig. 2(a) explains the fluctuation of the velocity profile along $x-$ direction due to the escalating of the constant parameter a. It has been distinguished that the velocity profile in $x-$ direction rises when the constant parameter a is rises. In $x-$ direction, the change in nanoliquid velocity due to the intensification of M is analyzed in Fig. 2(b). In this inquiry, enhancing behavior of the velocity profile in $x-$ direction is examined due to the growing values of M. The result of R on the nanoliquid velocity in $x-$ direction is inspected in Fig. 2(c). In Fig. 2(c), it has been detected that the intensification in rotating parameter R increases the fluid velocity profile along $x-$ direction. Fig. 3 are deliberated to scrutinize the disparity of the velocity profile in $z-$ direction with respect to the higher values of the constant parameter a, magnetic parameter M and rotating parameter R. The change in the fluid velocity in $z-$ direction due to the rising estimates of the constant parameter a is reflected in Fig. 3(a). It is examined that the intensifying estimates of the constant parameter a amplified the velocity profile in $z-$ direction. The role of M over the nanofluid velocity profile in $z-$ direction is considered in Fig. 3(b). In this Figure, the declining role of the nanoliquid velocity in $z-$ direction is observed due to the intensifying M. Fig. 3(c) explicates the consequence of the rotating parameter R on the fluid velocity profile in $z-$ direction. The nanoliquid velocity profile is decayed when the rotating factor R increases. The impacts of the constant parameter a, Eckert number Ec, Brownian motion parameter Nb, thermophoresis parameter Nt, and thermal radiation parameter Rd on the temperature of the nanofluid is examined in Figs. 4 and 5. Fig. 4(a) explores the significance of the constant parameter a on the nanoliquid thermal profile. Here, the nanoliquid temperature profile reduces for greater estimates of the constant parameter a. Fig. 4(b) reflects the behavior of nanoliquid thermal profile due to the enhancement of Ec. In this graph, the nanoliquid thermal profile increases for expanding values of Ec. In physical point of view, the viscous force becomes dominant within the boundary layer that causes the frictional heating within the boundary layer due to the viscous nature of the liquid. So from this observation, it has been examined that the Eckert number and fluid temperature are directly proportional to each other. Therefore, the nanoliquid thermal profile becomes higher when Ec is higher. The role of Nb on the nanoliquid thermal profile is offered in Fig. 4(c). It is perceived that the augmentation in fluid temperature is examined due to the greater estimates of Nb. From the physical perspective, the collision of the nanoparticles becomes higher because the motion of the nanoparticles is amplifying due to the enhancement of Nb. During this process, the kinetic energy transformed into thermal energy which consequently upsurges the temperature profile of the liquid. Fig. 5(a) exhibits the relationship between the nanofluid temperature and the thermophoresis parameter Nt. It is apparent that the increment in fluid temperature is observed due to the enhancement of Nt. Due to the enhancement of Nt, the transmission of heat becomes maximum because during this process heat diffusion becomes faster. So that the nanoliquid thermal profile is augmented through the intensification of the thermal boundary layer

Table 1
Comparison of the present outcomes with published results when all other parameters are zero.

a	C_{fx}			C_{fz}			Nu_x		
	Malvandi [61]	Ramesh et al. [44]	Present results	Malvandi [61]	Ramesh et al. [44]	Present results	Malvandi [61]	Ramesh et al. [44]	Present results
0.5	0.79913	0.79921	0.79921	0.30339	0.30354	0.30354	0.467648	0.467656	0.467656
1.0	1.2828	1.28232	1.28232	0.64579	0.64585	0.64585	0.589527	0.589536	0.589536
2.0	1.9172	1.91845	1.91845	1.05415	1.05427	1.05427	0.779526	0.779538	0.779538

Table 2
Effects of a, R, and M on C_{fx}.

a	R	M	C_{fx}
0.1			1.202650
0.2			0.850402
0.3			0.694350
0.4			0.601325
	0.2		0.699370
	0.4		0.689329
	0.6		0.679288
	0.8		0.669246
		1.0	0.207023
		2.0	0.612869
		3.0	1.432761
		4.0	2.252652

Table 3
Effect of a on C_{fz}.

a	C_{fz}
0.1	1.362418
0.2	0.963375
0.3	0.786592
0.4	0.681209

Table 4
Effects of Rd, Ec, Nt and Nb on Nu_x.

Rd	Ec	Nt	Nb	Nu_x
1.0				1.598441
1.5				1.924126
2.0				2.220242
2.5				2.486788
	0.1			1.325685
	0.3			1.243185
	0.5			1.160685
	0.7			1.078185
		0.1		1.325685
		0.2		1.284435
		0.3		1.243185
		0.4		1.201935
			0.2	1.201935
			0.3	1.160685
			0.4	1.119435
			0.5	1.078185

Table 5
Effects of Nt, Nb and C_R on Sh_x.

Nt	Nb	C_R	Sh_x
0.1			0.656333
0.2			1.023000
0.3			1.389667
0.4			1.756333
	0.2		0.839667
	0.3		0.656333
	0.4		0.564667
	0.5		0.509667
		1.2	1.591333
		1.4	1.628000
		1.6	1.664667
		1.8	1.701333

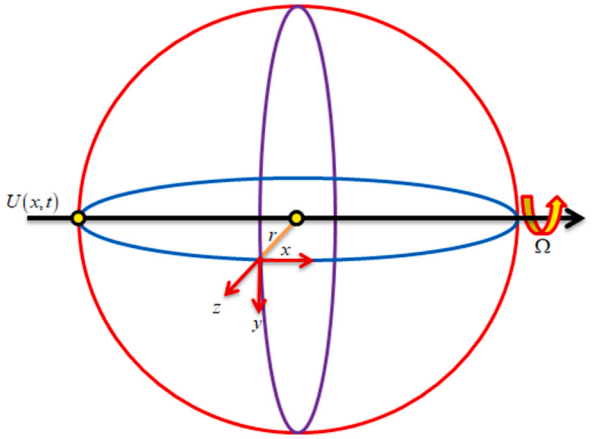

Fig. 1. Geometry of the flow problem.

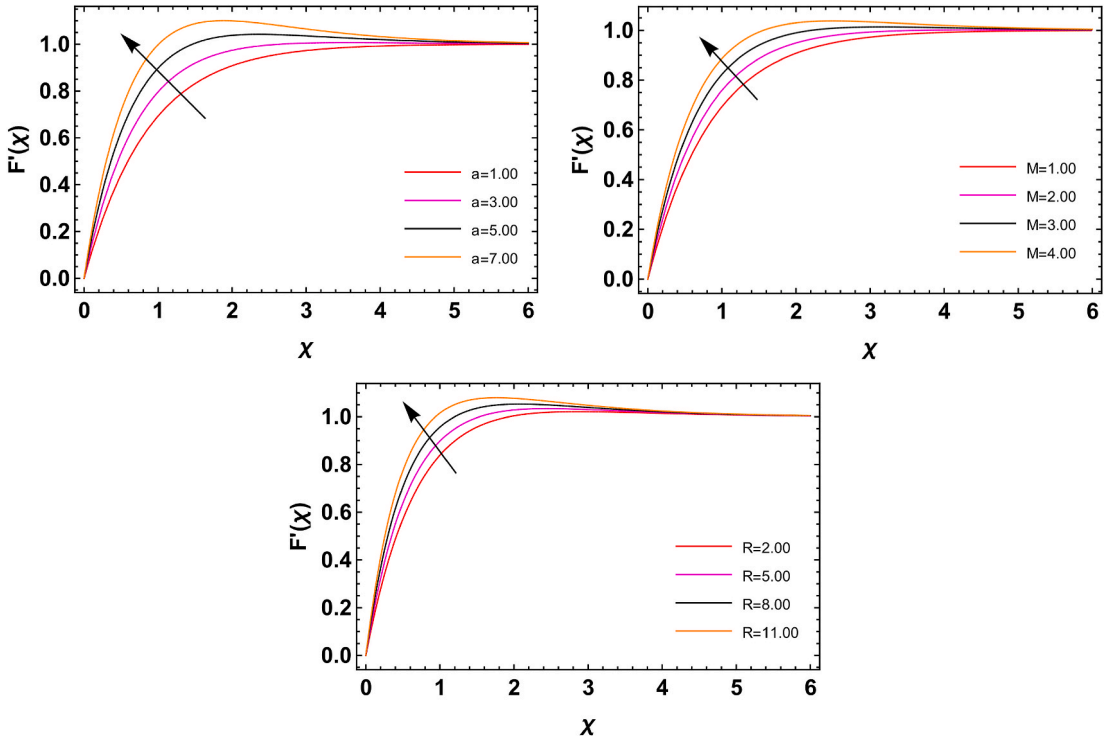

Fig. 2. (A): Fluctuation in velocity profile due to *a*. (b): Fluctuation in velocity profile due to *M*. (c): Fluctuation in velocity profile due to *R*.

thickness. Fig. 5(b) displays the role of *Rd* on the thermal profile of the nanofluid. It is observed that the boosting values of *Rd* boosted the nanoliquid thermal profile. The relative contribution of heat transfer conduction to the thermal radiation heat transfer is known as the thermal radiation. The conduction of heat transfer is dominant over the thermal radiation heat transfer in case of $Rd > 1$. Therefore, the magnitude of the thermal boundary layer thickness and fluid temperature are rises as the values of the thermal radiation parameter increases. Figs. 6 and 7 signify the consequence of the constant parameter *a*, chemical reaction parameter C_R, thermophoresis parameter *Nt*, and Schmidt number *Sc* on the concentration of the fluid. Fig. 6(a) expresses the disparity in nanoliquid concentration profile for amplifying estimates of the constant parameter *a*. In this Figure, it is interpreted that the decrement behavior of the fluid concentration is observed for amplified values of constant parameter *a*. Fig. 6(b) highlights the physical behavior of the C_R on the nanofluid solutal profile. It is examined that the larger C_R declines the nanoliquid concentration profile. Further, with the rise of C_R, the liquid molecular diffusivity reduces which consequently declines the fluid solutal profile. Fig. 6(c) is capture to scrutinize the significance of *Nt* on the solutal profile of the fluid. It is observed that the fluid concentration becomes higher and higher due to the change of *Nt*. It is noticed that insides the flow regime thermophoresis forces are increases as the thermophoresis parameter rises.

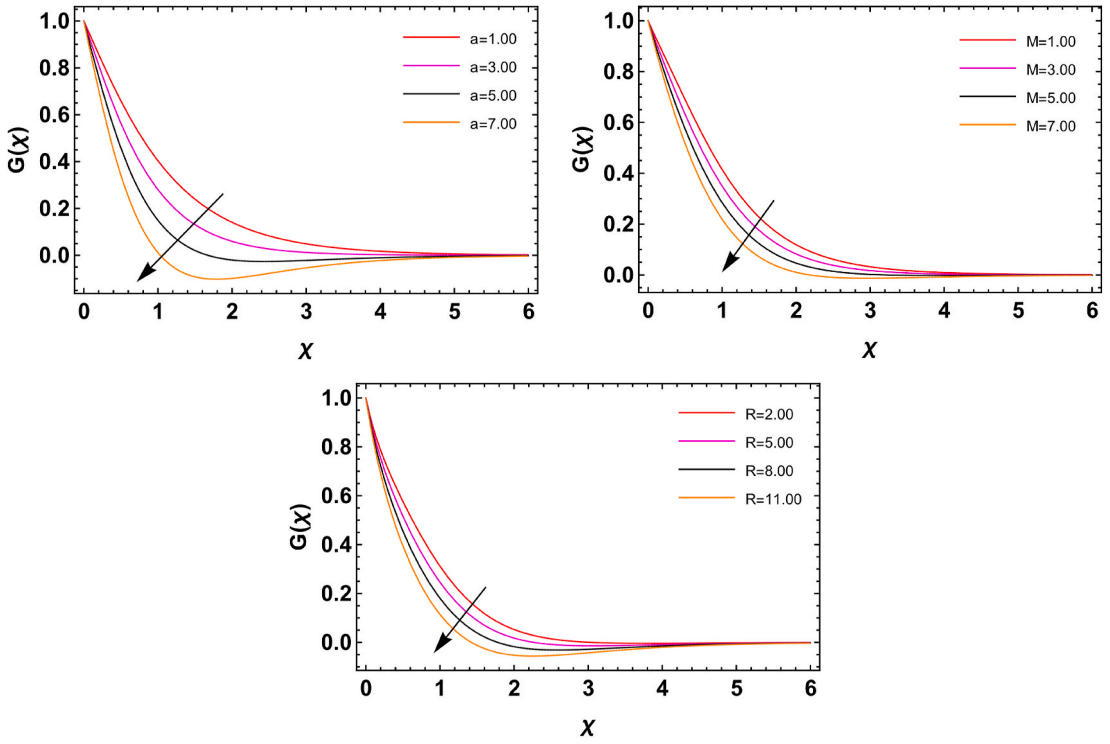

Fig. 3. (A): Fluctuation in velocity profile due to *a*. 3(b): Fluctuation in velocity profile due to *M*. (c): Fluctuation in velocity profile due to *R*.

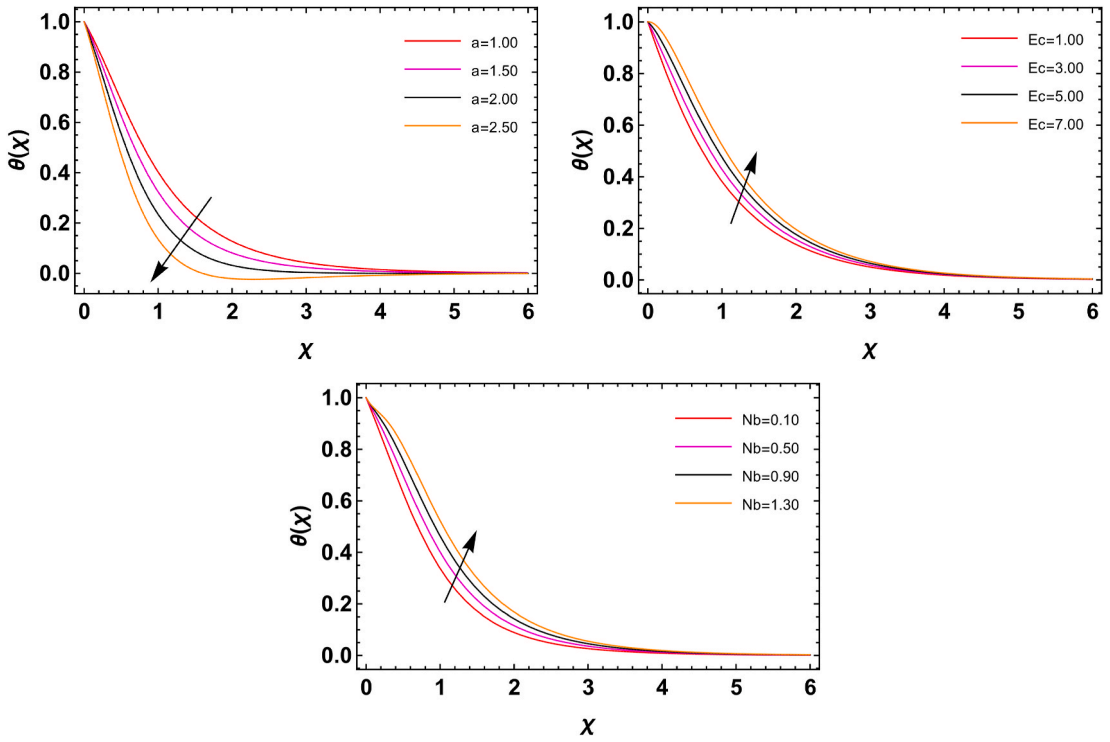

Fig. 4. (A): Fluctuation in temperature profile due to *a*. (b): Fluctuation in temperature profile due to *Ec*. (c): Fluctuation in temperature profile due to *Nb*.

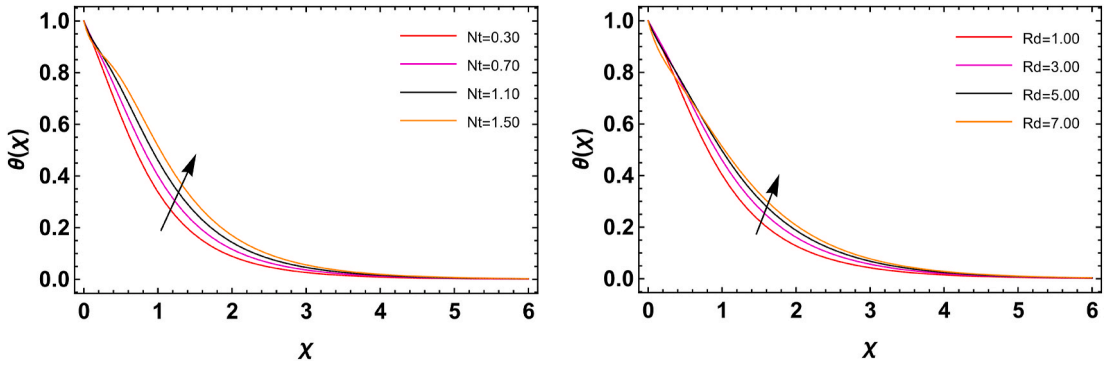

Fig. 5. (A): Fluctuation in temperature profile due to *Nt*. (b): Fluctuation in temperature profile due to *Rd*.

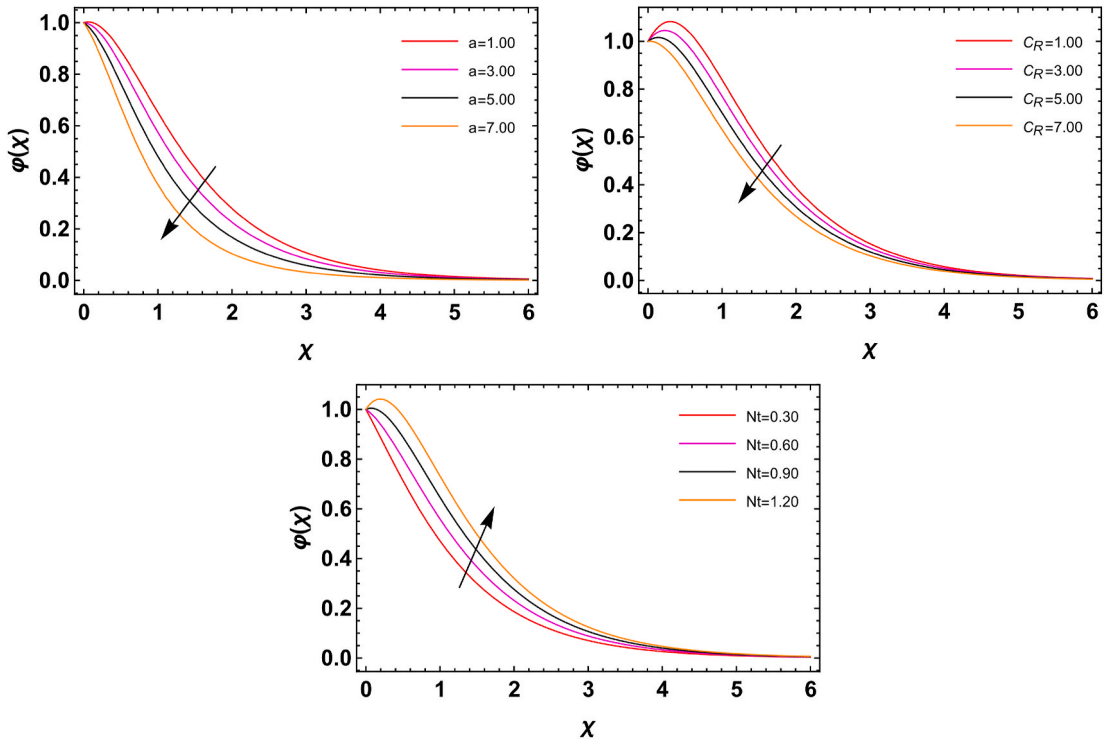

Fig. 6. (A): Fluctuation in concentration profile due to *a*. 6(b): Fluctuation in concentration profile due to C_R. (c): Fluctuation in concentration profile due to *Nt*.

Therefore, the nanoliquid solutal profile increases with the amplifying thermophoresis parameter. The outcome of *Sc* on the nanoliquid concentration is discussed in Fig. 7. From this observation, the declining role of the fluid concentration is examined for the higher *Sc*. Moreover, the mass transport rises but the solutal boundary layer thickness diminishes due to the amplifying *Sc*. As a result, the liquid concentration decayed when *Sc* increases.

5. Conclusion

The authors have investigated the MHD flow of a nanoliquid due to the rotating sphere at a stagnation point in this study. The flow is considered to be influenced by the magnetic field, dissipative, thermally radiative and chemically reactive. Also, the Brownian and thermal diffusivity influences are taken into consideration. Some restrictions in the present analysis are taken: like there is no-slip and convective conditions, joule heating, Hall effects and buoyancy-driven. The simulation of the existing model is done with the applying of HAM scheme. The outcomes of the present analysis are displayed in the form of Tables and Figures. At the end of this study, the authors have found some important results which are listed as.

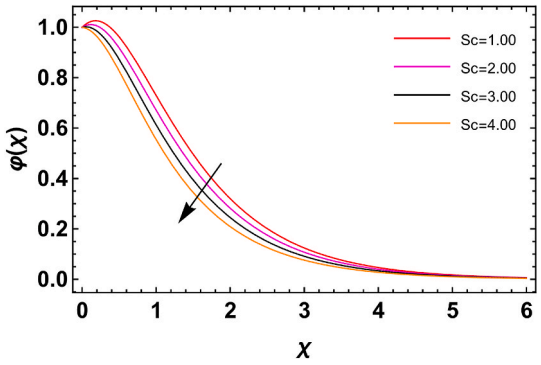

Fig. 7. Fluctuation in concentration profile due to *Sc*.

- The increasing rotation, magnetic and positive constant parameters have increased the velocity profiles along the *x*-direction, while reduced the velocity profiles along the z-direction.
- The rising effect of *a* diminishes the thermal profile. While the increasing Eckert number, thermophoresis, Brownian motion, and thermal radiation factor have escalated the thermal profiles of the nanoliquid flow.
- The expanding positive constant, chemical reaction factor and Schmidt number have decayed the solutal profiles. The increasing thermophoresis factor has an augmenting impact on the solutal profiles.
- The declination of skin friction in *x*-direction is noted for greater values of the constant parameter, rotating parameter, and magnetic field parameter. It is also eminent that with the amplification of the constant parameter, the skin friction coefficient in y-direction has declined.
- The Nusselt number is lower for higher Eckert number, thermophoresis parameter, and Brownian motion parameter, while the increment in thermal radiation parameter augmented the Nusselt number.
- It is perceived that the nanoliquid Sherwood number enhances due to the intensification of the thermophoresis parameter and chemical reaction parameter. Further, the decayed behavior of the Sherwood number of the nanoliquid is noted when the Brownian motion parameter enhances.

Funding information

The authors acknowledge the financial support provided by the Center of Excellence in Theoretical and Computational Science (TaCS-CoE), KMUTT. This research was funded by National Science, Research and Innovation Fund (NSRF), King Mongkut's University of Technology North Bangkok with Contract no. KMUTNB-FF-66-36.

Author contribution statement

Showkat Ahmad Lone: Analyzed and interpreted the data; Wrote the paper.
Sadia Anwar; Anwar Saeed: Conceived and designed the experiments.
Zehba Raizah: Contributed analysis tools or data; Wrote the paper.
Poom Kumam: Analyzed and interpreted the data.
Thidaporn Seangwattana: Contributed analysis tools or data.

Data availability statement

Data will be made available on request.

Declaration of competing interest

The authors declare that they have no known competing financial interests or personal relationships that could have appeared to influence the work reported in this paper

References

[1] M.I. Asjad, M.D. Ikram, A. Akgül, Analysis of MHD viscous fluid flow through porous medium with novel power law fractional differential operator, Phys. Scripta 95 (2020), 115209.
[2] H. Vaidya, C. Rajashekhar, B.B. Divya, G. Manjunatha, K.V. Prasad, I.L. Animasaun, Influence of transport properties on the peristaltic MHD Jeffrey fluid flow through a porous asymmetric tapered channel, Results Phys. 18 (2020), 103295, https://doi.org/10.1016/J.RINP.2020.103295.
[3] M.V. Reddy, L. Pallavarapu, K. Vajravelu, A comparative study of MHD non-Newtonian fluid flows with the effects of chemical reaction and radiation over a stretching sheet, Comput. Therm. Sci. An Int. J. 13 (2021).

[4] W. Fenizri, M. Kezzar, M.R. Sari, I. Tabet, M.R. Eid, New modified decomposition method (DRMA) for solving MHD viscoelastic fluid flow: comparative study, Int. J. Ambient Energy (2020) 1–9.

[5] R. Ali, A. Shahzad, K. us Saher, Z. Elahi, T. Abbas, The thin film flow of Al2O3 nanofluid particle over an unsteady stretching surface, Case Stud. Therm. Eng. 29 (2022), 101695.

[6] M. Saeed, B. Ahmad, T. Abbas, M.I. Khan, S.U. Khan, Consequences of Thermal Slip Flow of Non-newtonian Fluid with Temperature-dependent Thermal Conductivity, Waves in Random and Complex Media, 2022, pp. 1–19.

[7] N.W. Khan, A. Khan, M. Usman, T. Gul, A. Mouldi, A. Brahmia, Influences of Marangoni convection and variable magnetic field on hybrid nanofluid thin-film flow past a stretching surface, Chin. Phys. B 31 (2022), 64403.

[8] R. Kodi, O. Mopuri, Unsteady MHD oscillatory Casson fluid flow past an inclined vertical porous plate in the presence of chemical reaction with heat absorption and Soret effects, Heat Transf. 51 (2022) 733–752.

[9] K.U. Rehman, W. Shatanawi, Q.M. Al-Mdallal, A comparative remark on heat transfer in thermally stratified MHD Jeffrey fluid flow with thermal radiations subject to cylindrical/plane surfaces, Case Stud. Therm. Eng. 32 (2022), 101913.

[10] T. Abbas, B. Ahmad, A. Majeed, T. Muhammad, M. Ismail, Numerical investigations of radiative flow of viscous fluid through porous medium, Jpn. Mag. 26 (2021) 277–284.

[11] T. Abbas, A. Majeed, B. Ahmad, M. Noveel Sadiq, Q.M. Ul Hassan, H. Ullah, S.M. Al-Mekhlafi, Dual solution with heat transfer through moving porous plate of an unsteady incompressible viscous fluid, J. Chem. 2022 (2022).

[12] A.S. Mittal, H.R. Patel, Influence of thermophoresis and Brownian motion on mixed convection two dimensional MHD Casson fluid flow with non-linear radiation and heat generation, Phys. A Stat. Mech. Appl. 537 (2020), 122710.

[13] A. Riaz, Q.M.U. Hassan, T. Abbas, K. Ghachem, A. Majeed, F.M. Noori, L. Kolsi, A study on effectiveness of the variational theory in fluid dynamics applications, Alex. Eng. J. 61 (2022) 10779–10789.

[14] Z. Sabir, A. Ayub, J.L.G. Guirao, S. Bhatti, S.Z.H. Shah, The effects of activation energy and thermophoretic diffusion of nanoparticles on steady micropolar fluid along with Brownian motion, Adv. Mater. Sci. Eng. 2020 (2020).

[15] K. Guedri, A. Khan, N. Sene, Z. Raizah, A. Saeed, A.M. Galal, Thermal flow for radiative ternary hybrid nanofluid over nonlinear stretching sheet subject to Darcy–forchheimer phenomenon, Math. Probl Eng. 2022 (2022).

[16] S.I. Abdelsalam, K.S. Mekheimer, A.Z. Zaher, Dynamism of a Hybrid Casson Nanofluid with Laser Radiation and Chemical Reaction through Sinusoidal Channels, Waves in Random and Complex Media, 2022, pp. 1–22.

[17] V. Sridhar, K. Ramesh, M. Gnaneswara Reddy, M.N. Azese, S.I. Abdelsalam, On the Entropy Optimization of Hemodynamic Peristaltic Pumping of a Nanofluid with Geometry Effects, Waves in Random and Complex Media, 2022, pp. 1–21.

[18] U. Khan, S. Bilal, A. Zaib, O.D. Makinde, A. Wakif, Numerical simulation of a nonlinear coupled differential system describing a convective flow of Casson gold–blood nanofluid through a stretched rotating rigid disk in the presence of Lorentz forces and nonlinear thermal radiation, Numer. Methods Part. Differ. Equ. (2020), https://doi.org/10.1002/NUM.22620.

[19] F. Mabood, M.D. Shamshuddin, S.R. Mishra, Characteristics of thermophoresis and Brownian motion on radiative reactive micropolar fluid flow towards continuously moving flat plate: HAM solution, Math. Comput. Simulat. 191 (2022) 187–202.

[20] H. Upreti, A.K. Pandey, Z. Uddin, M. Kumar, Thermophoresis and Brownian motion effects on 3D flow of Casson nanofluid consisting microorganisms over a Riga plate using PSO: a numerical study, Chin. J. Phys. 78 (2022) 234–270.

[21] H.U. Rasheed, W. Khan, I. Khan, N. Alshammari, N. Hamadneh, Numerical computation of 3D Brownian motion of thin film nanofluid flow of convective heat transfer over a stretchable rotating surface, Sci. Rep. 12 (2022) 1–14.

[22] H.U. Rasheed, S. Islam, Zeeshan, T. Abbas, J. Khan, Analytical treatment of MHD flow and chemically reactive Casson fluid with Joule heating and variable viscosity effect, Waves Random Complex Media (2022) 1–17.

[23] G.M. Shaikh Zeeshan, Analysis of temperature-dependent viscosity effect on wire coating using MHD flow of incompressible third-grade nanofluid filled in cylindrical coating die, Adv. Mech. Eng. 14 (2022), 16878132221089172.

[24] G. Rasool, A. Shafiq, D. Baleanu, Consequences of Soret–Dufour effects, thermal radiation, and binary chemical reaction on Darcy Forchheimer flow of nanofluids, Symmetry 12 (2020) 1421.

[25] Z. Khan, H.U. Rasheed, I. Khan, H. Abu-Zinadah, M.A. Aldahlan, Mathematical simulation of casson MHD flow through a permeable moving wedge with nonlinear chemical reaction and nonlinear thermal radiation, Materials 15 (2022) 747.

[26] N.A. Zainal, R. Nazar, K. Naganthran, I. Pop, Flow and heat transfer over a permeable moving wedge in a hybrid nanofluid with activation energy and binary chemical reaction, Int. J. Numer. Methods Heat Fluid Flow (2021).

[27] J. Cui, R. Razzaq, U. Farooq, W.A. Khan, F.B. Farooq, T. Muhammad, Impact of non-similar modeling for forced convection analysis of nano-fluid flow over stretching sheet with chemical reaction and heat generation, Alex. Eng. J. 61 (2022) 4253–4261.

[28] R. Raza, R. Naz, S.I. Abdelsalam, Microorganisms swimming through radiative Sutterby nanofluid over stretchable cylinder: hydrodynamic effect, Numer. Methods Part. Differ. Equ. 39 (2023) 975–994.

[29] M. Faizan, F. Ali, K. Loganathan, A. Zaib, C.A. Reddy, S.I. Abdelsalam, Entropy analysis of Sutterby nanofluid flow over a Riga sheet with gyrotactic microorganisms and cattaneo–christov double diffusion, Mathematics 10 (2022) 3157.

[30] T. Salahuddin, Z. Mahmood, M. Khan, M. Awais, A permeable squeezed flow analysis of Maxwell fluid near a sensor surface with radiation and chemical reaction, Chem. Phys. 562 (2022), 111627.

[31] D. Dey, R. Borah, A.S. Khound, Stability analysis on dual solutions of MHD Casson fluid flow with thermal and chemical reaction over a permeable elongating sheet, Heat Transf. 51 (2022) 3401–3417.

[32] Zeeshan, Heat Enhancement Analysis of Maxwell Fluid Containing Molybdenum Disulfide and Graphene Nanoparticles in Engine Oil Base Fluid with Isothermal Wall Temperature Conditions, Waves in Random and Complex Media, 2023, pp. 1–15.

[33] H.U. Rasheed, S. Islam, Zeeshan, W. Khan, J. Khan, T. Abbas, Numerical modeling of unsteady MHD flow of Casson fluid in a vertical surface with chemical reaction and Hall current, Adv. Mech. Eng. 14 (2022), 16878132221085428.

[34] F. Wang, S.A. Khan, S. Gouadria, E.R. El-Zahar, M.I. Khan, S.U. Khan, M. Yasir, Y.-M. Li, Entropy optimized flow of Darcy-Forchheimer viscous fluid with cubic autocatalysis chemical reactions, Int. J. Hydrogen Energy 47 (2022) 13911–13920.

[35] G. Lakshmi Devi, H. Niranjan, S. Sivasankaran, Effects of chemical reactions, radiation, and activation energy on MHD buoyancy induced nano fluidflow past a vertical surface, Sci. Iran. 29 (2022) 90–100.

[36] A. Khan, W. Kumam, I. Khan, A. Saeed, T. Gul, P. Kumam, I. Ali, Chemically reactive nanofluid flow past a thin moving needle with viscous dissipation, magnetic effects and hall current, PLoS One 16 (2021), e0249264.

[37] R. Mohana Ramana, K. Venkateswara Raju, K. Raghunath, Chemical reaction with aligned magnetic field effects on unsteady MHD Kuvshinski fluid flow past an inclined porous plate in the presence of radiation and Soret effects, Heat Transf. (2022).

[38] S.U. Haq, S.U. Jan, R. Bilal, J.H. Alzahrani, I. Khan, A. Alzahrani, Heat-mass transfer of MHD second grade fluid flow with exponential heating, chemical reaction and porosity by using fractional Caputo-Fabrizio derivatives, Case Stud. Therm. Eng. 36 (2022), 102104.

[39] Y. Yin, W. Chen, C. Wu, X. Zhang, T. Fu, C. Zhu, Y. Ma, Bubble dynamics and mass transfer enhancement in split–and–recombine (SAR) microreactor with rapid chemical reaction, Sep. Purif. Technol. 287 (2022), 120573.

[40] A. Mahdy, A.J. Chamkha, H.A. Nabwey, Entropy analysis and unsteady MHD mixed convection stagnation-point flow of Casson nanofluid around a rotating sphere, Alex. Eng. J. 59 (2020) 1693–1703.

[41] A. Mahdy, H.A. Nabwey, Microorganisms time-mixed convection nanofluid flow by the stagnation domain of an impulsively rotating sphere due to Newtonian heating, Results Phys. 19 (2020), 103347, https://doi.org/10.1016/J.RINP.2020.103347.

[42] B. Ali, A. Shafiq, A. Manan, A. Wakif, S. Hussain, Bioconvection: significance of mixed convection and mhd on dynamics of Casson nanofluid in the stagnation point of rotating sphere via finite element simulation, Math. Comput. Simulat. 194 (2022) 254–268.

[43] P.M. Patil, S. Benawadi, B. Shanker, Influence of mixed convection nanofluid flow over a rotating sphere in the presence of diffusion of liquid hydrogen and ammonia, Math. Comput. Simulat. 194 (2022) 764–781.
[44] G.K. Ramesh, J.K. Madhukesh, N.A. Shah, S.-J. Yook, Flow of hybrid CNTs past a rotating sphere subjected to thermal radiation and thermophoretic particle deposition, Alex. Eng. J. (2022).
[45] A. Dawar, N. Acharya, Unsteady mixed convective radiative nanofluid flow in the stagnation point region of a revolving sphere considering the influence of nanoparticles diameter and nanolayer, J. Indian Chem. Soc. (2022), 100716, https://doi.org/10.1016/J.JICS.2022.100716.
[46] Z. Mahmood, S.E. Alhazmi, U. Khan, M.Z. Bani-Fwaz, A.M. Galal, Unsteady MHD stagnation point flow of ternary hybrid nanofluid over a spinning sphere with Joule heating, Int. J. Mod. Phys. B (2022), 2250230.
[47] N. Abbas, K.U. Rehman, W. Shatanawi, M.Y. Malik, Numerical study of heat transfer in hybrid nanofluid flow over permeable nonlinear stretching curved surface with thermal slip, Int. Commun. Heat Mass Tran. 135 (2022), 106107, https://doi.org/10.1016/J.ICHEATMASSTRANSFER.2022.106107.
[48] N. Abbas, W. Shatanawi, T.A.M. Shatnawi, Theoretical analysis of modified non-Newtonian micropolar nanofluid flow over vertical Riga sheet, Int. J. Mod. Phys. B 37 (2023), 2350016.
[49] N. Abbas, W. Shatanawi, K.U. Rehman, T.A.M. Shatnawi, Velocity and thermal slips impact on boundary layer flow of micropolar nanofluid over a vertical nonlinear stretched Riga sheet, Proc. Inst. Mech. Eng. Part N J. Nanomater. Nanoeng. Nanosyst. (2023), 23977914231156684.
[50] K.V.B. Rajakumar, M. Umasankara Reddy, K.S. Balamurugan, K. Raja Ram, Steady MHD Casson Ohmic heating and viscous dissipative fluid flow past an infinite vertical porous plate in the presence of Soret, Hall, and ion-slip current, Heat Transf. 49 (2020) 1583–1612.
[51] A.M. Megahed, M.G. Reddy, Numerical treatment for MHD viscoelastic fluid flow with variable fluid properties and viscous dissipation, Indian J. Phys. 95 (2021) 673–679.
[52] D. Gopal, S. Saleem, S. Jagadha, F. Ahmad, A.O. Almatroud, N. Kishan, Numerical analysis of higher order chemical reaction on electrically MHD nanofluid under influence of viscous dissipation, Alex. Eng. J. 60 (2021) 1861–1871.
[53] W. Abbas, A.M. Megahed, Numerical solution for chemical reaction and viscous dissipation phenomena on non-Newtonian MHD fluid flow and heat mass transfer due to a nonuniform stretching sheet with thermal radiation, Int. J. Mod. Phys. C 32 (2021), 2150124.
[54] S. Nadeem, M. Tumreen, B. Ishtiaq, N. Abbas, W. Shatanawi, Second-grade nanofluid flow above a vertical slandering Riga surface with double diffusion model, Int. J. Mod. Phys. B 36 (2022), 2250237.
[55] W. Shatanawi, N. Abbas, T.A.M. Shatnawi, F. Hasan, Heat and mass transfer of generalized fourier and Fick's law for second-grade fluid flow at slendering vertical Riga sheet, Heliyon 9 (2023).
[56] M. Yaseen, S.K. Rawat, M. Kumar, Hybrid nanofluid (MoS2–SiO2/water) flow with viscous dissipation and Ohmic heating on an irregular variably thick convex/concave-shaped sheet in a porous medium, Heat Transf. 51 (2022) 789–817.
[57] H.R. Kataria, M. Mistry, A. Mittal, Influence of nonlinear radiation on MHD micropolar fluid flow with viscous dissipation, Heat Transf. 51 (2022) 1449–1467.
[58] K. Sharma, S. Kumar, N. Vijay, Numerical simulation of MHD heat and mass transfer past a moving rotating disk with viscous dissipation and ohmic heating, Multidiscip. Model. Mater. Struct. (2022).
[59] M.M. Bhatti, S.I. Abdelsalam, Scientific breakdown of a ferromagnetic nanofluid in hemodynamics: enhanced therapeutic approach, Math. Model Nat. Phenom. 17 (2022) 44.
[60] D. Anilkumar, S. Roy, Self-similar solution of the unsteady mixed convection flow in the stagnation point region of a rotating sphere, Heat Mass Tran. 40 (2004) 487–493.
[61] A. Malvandi, The unsteady flow of a nanofluid in the stagnation point region of a time-dependent rotating sphere, Therm. Sci. 19 (2015) 1603–1612.